C4orf41 and TTC-15 are mammalian TRAPP components with a role at an early stage in ER-to-Golgi trafficking

P. James Scrivens[a], Baraa Noueihed[a,*], Nassim Shahrzad[a], Sokunthear Hul[a], Stephanie Brunet[a], and Michael Sacher[a,b]

[a]Department of Biology, Concordia University, Montreal, Quebec, Canada; [b]Department of Anatomy and Cell Biology, McGill University, Montreal, Quebec, Canada

ABSTRACT **TRAPP is a multisubunit tethering complex implicated in multiple vesicle trafficking steps in *Saccharomyces cerevisiae* and conserved throughout eukarya, including humans. Here we confirm the role of TRAPPC2L as a stable component of mammalian TRAPP and report the identification of four novel components of the complex: C4orf41, TTC-15, KIAA1012, and Bet3L. Two of the components, KIAA1012 and Bet3L, are mammalian homologues of Trs85p and Bet3p, respectively. The remaining two novel TRAPP components, C4orf41 and TTC-15, have no homologues in *S. cerevisiae*. With this work, human homologues of all the *S. cerevisiae* TRAPP proteins, with the exception of the *Saccharomycotina*-specific subunit Trs65p, have now been reported. Through a multidisciplinary approach, we demonstrate that the novel proteins are bona fide components of human TRAPP and implicate C4orf41 and TTC-15 (which we call TRAPPC11 and TRAPPC12, respectively) in ER-to-Golgi trafficking at a very early stage. We further present a binary interaction map for all known mammalian TRAPP components and evidence that TRAPP oligomerizes. Our data are consistent with the absence of a TRAPP I–equivalent complex in mammalian cells, suggesting that the fundamental unit of mammalian TRAPP is distinct from that characterized in *S. cerevisiae*.**

Monitoring Editor
Francis A. Barr
University of Liverpool

Received: Nov 19, 2010
Revised: Apr 14, 2011
Accepted: Apr 20, 2011

INTRODUCTION

Eukaryotic intracellular vesicle trafficking requires a suite of molecular activities to ensure appropriate targeting of the vesicle and its contents. These activities include sorting, budding, movement, tethering, and fusion of the vesicle, with each step adding a layer of specificity to the trafficking process (Bonifacino and Glick, 2004). *Saccharomyces cerevisiae* TRAPP is a multisubunit tethering complex, with two distinct forms called TRAPP I and TRAPP II, implicated in endoplasmic reticulum (ER) to Golgi and late Golgi trafficking, respectively (Sacher *et al.*, 2001; Cai *et al.*, 2005). Although TRAPP is conserved in all eukaryotes, the function and composition of mammalian TRAPP are not well characterized. It is notable that mutation in the human orthologue of Trs20p, TRAPPC2/sedlin, is the causative lesion in X-linked spondyloepiphyseal dysplasia tarda (SEDT) (Gedeon *et al.*, 1999, 2001; Tiller *et al.*, 2001; Shaw *et al.*, 2003).

S. cerevisiae TRAPP I consists of Bet5p, Trs20p, Bet3p, Trs23p, Trs31p, and Trs33p (Sacher *et al.*, 1998, 2000, 2001), with the mammalian orthologues named TRAPPC1, TRAPPC2, TRAPPC3, TRAPPC4, TRAPPC5, and TRAPPC6a/b, respectively (Sacher *et al.*, 2008) (see Table 1 for nomenclature used in this paper). *S. cerevisiae* Trs85p associates with TRAPP I but has recently been proposed to form a distinct subcomplex with a role in autophagy (Nazarko *et al.*, 2005; Meiling-Wesse *et al.*, 2005; Lynch-Day *et al.*, 2010). TRAPP II consists of the TRAPP I "core," with the additional subunits Trs65p, Trs120p, and Trs130p (Sacher *et al.*, 2001). A recently characterized protein, Tca17p, may associate specifically with TRAPP II (Montpetit and Conibear, 2009; Scrivens *et al.*, 2009). The *S. cerevisiae* TRAPP I and TRAPP II complexes are stable assemblies that fractionate discretely in size-exclusion chromatography. In contrast, upon size

This article was published online ahead of print in MBoC in Press (http://www.molbiolcell.org/cgi/doi/10.1091/mbc.E10-11-0873) on April 27, 2011.

*Present address: Department of Pharmacology and Therapeutics, McGill University, Montreal, Quebec, Canada.

Abbreviations used: EGF, epidermal growth factor; ER, endoplasmic reticulum; ERGIC, ER-Golgi intermediate compartment; Man II, alpha-mannosidase II; SEDT, spondyloepiphyseal dysplasia tarda; TAP, tandem affinity purification; Tfn, transferrin; TRAPP, Transport Protein Particle; VSV-G, vesicular stomatitis virus glycoprotein.

Address correspondence to: Michael Sacher (msacher@alcor.concordia.ca).

S. cerevisiae TRAPP subunit (kDa)	Mammalian TRAPP subunit (kDa)
Bet5p (18)	TRAPPC1 (17)
Tca17p (17)	TRAPPC2L (16)
Trs20p (20)	TRAPPC2 (16)
Bet3p (22)	TRAPPC3, TRAPPC3L* (20)
Trs23p (23)	TRAPPC4 (24)
Trs31p (31)	TRAPPC5 (21)
Trs33p (33)	TRAPPC6a,b (19,15)
Trs65p (65)	
Trs85p (85)	TRAPPC8* (161)
Trs120p (120)	TRAPPC9 (140)
Trs130p (130)	TRAPPC10 (142)
	TRAPPC11* (129)
	TRAPPC12* (79)

*Reported in this study; see Table 2 for accession numbers.
Proteins on the same row indicate homologues; empty cells indicate no homologues detected in databases.

TABLE 1: Mammalian and yeast TRAPP subunit nomenclature.

exclusion chromatography, mammalian TRAPP proteins elute as a single high-molecular-weight complex, suggesting the absence of a small complex equivalent to TRAPP I (Loh *et al.*, 2005; Scrivens *et al.*, 2009; Yamasaki *et al.*, 2009).

The functions of the yeast TRAPP I complex are well-defined. In addition to its role as a COP II–vesicle tethering factor (Sacher *et al.*, 2001), the complex acts as a guanine nucleotide exchange factor (GEF) for Ypt1p (Wang *et al.*, 2000). These activities are dependent on the subunits Bet3p, Trs31p, Trs23p, and Bet5p (Kim *et al.*, 2006; Cai *et al.*, 2007). Functions have yet to be definitively assigned to the remainder of the subunits, although it has been suggested that Trs120p and Trs130p switch the GEF activity from Ypt1p to Ypt31/32p (Morozova *et al.*, 2006). Direct demonstration of mammalian TRAPP as a vesicle tether has yet to be shown, but it has recently been reported to stimulate nucleotide exchange on the Ypt1p-related protein Rab1 (Yamasaki *et al.*, 2009).

We recently used a bioinformatic approach to identify a novel TRAPP-interacting protein, TRAPPC2L (for simplicity, mammalian subunits will henceforth be referred to without the "TRAPP" prefix) (Scrivens *et al.*, 2009). The protein displays homology to yeast Trs20p and a previously uncharacterized open reading frame YEL048c/*TCA17* (Montpetit and Conibear, 2009; Scrivens *et al.*, 2009). C2L cofractionated with the mammalian TRAPP complex and its depletion with small interfering RNA (siRNA) led to an identical Golgi fragmentation phenotype to that seen upon C2 knockdown, supporting the hypothesis that C2L is a component of mammalian TRAPP. Here we have used tandem affinity purification (TAP)-tagged C2 and C2L coupled to mass spectrometry to demonstrate that both proteins are found in stable TRAPP complexes in mammalian cells. As well as the mammalian TRAPP I orthologues listed above, we find that C2 and C2L stably associate with a putative Trs85p orthologue, KIAA1012, which we here refer to as C8. Both also associate with the previously reported Trs120p and Trs130p orthologues, NIBP (C9) and TMEM1 (C10) (Cox *et al.*, 2007). In addition, here we report two novel TRAPP proteins, C4orf41/Gryzun (now designated TRAPPC11) and TTC-15 (now designated TRAPPC12) that, while being found throughout eukarya including diverse fungi, are absent in *S. cerevisiae*. Whereas Trs85p was recently implicated in autophagy in *S. cerevisiae*, we provide evidence that the mammalian Trs85p orthologue C8, as well as C11 and C12, are bona fide TRAPP components with roles in ER-to-Golgi trafficking. Specifically, we implicate C11 in membrane traffic between the ER and the ERGIC compartment. Using a combination of binary yeast two-hybrid analysis and biochemical studies, we provide evidence that TRAPP oligomerizes and present an initial model of the architecture of mammalian TRAPP. Our study suggests the absence of a TRAPP I subcomplex in mammalian cells and implies fundamental differences between *S. cerevisiae* and mammals in how TRAPP regulates early secretory pathway trafficking.

RESULTS

TAP-tagged C2 and C2L identify new TRAPP interactors in human cells

The yeast orthologue of C2L, Tca17p, was shown to associate loosely with TRAPP and implied, based in part on yeast genetic interactions, to have a TRAPP II–specific function (Montpetit and Conibear, 2009; Scrivens *et al.*, 2009). In an effort to discern a functional difference between C2 and C2L, we precipitated tandem affinity purification (TAP)-tagged C2 and C2L followed by SDS–PAGE and mass spectrometry. Somewhat surprisingly, the pattern of associated bands detected by silver staining was essentially indistinguishable between the two proteins, suggesting that the two proteins are found in equivalent complexes (Figure 1A). The presence of C2 and C2L in the same complex was indeed confirmed as seen by the coprecipitation of myc-tagged C2 with FLAG-tagged C2L (Figure 1B), consistent with the notion that C2L completes the symmetry of the TRAPP core, residing opposite C2, as previously suggested (Scrivens *et al.*, 2009).

Analysis of the C2- and C2L-interacting proteins demonstrated the presence of known human TRAPP components, including C3, C4, and C5, as well as the previously reported yeast TRAPP II orthologues C9 and C10 (see Figure 1C). Several novel, high-molecular-weight proteins were also identified in the purifications (Figure 1A and Table 2). Peptides originating from KIAA1012, TTC-15, and C4orf41 (the human orthologue of *Drosophila melanogaster* Gryzun and *Danio rerio* Foie gras) were detected. These proteins have not been previously characterized as TRAPP components, but KIAA1012 was annotated in GenBank as TRAPPC8, a Trs85p orthologue. Interestingly, C4orf41/gryzun was recently identified in a *D. melanogaster* screen as a novel component involved in secretion (Wendler *et al.*, 2010). Given that C9 and C4orf41 comigrate,

Protein name	GenBank accession number	TRAPP subunit	No. peptides detected in all TAP purifications	Molecular size (kDa)
KIAA1012	NP_055754.2	TRAPPC8	88	161
C4orf41	NP_068761.4	TRAPPC11	69	129
TTC-15	NP_057114.5	TRAPPC12	35	79

TABLE 2: TRAPP subunits identified by proteomics.

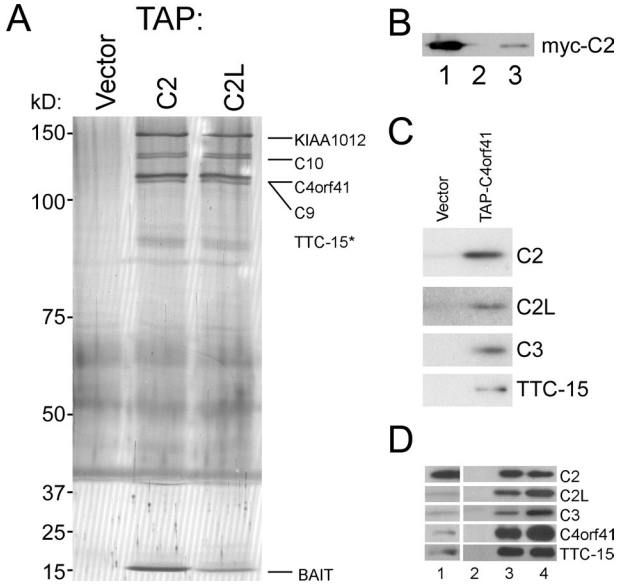

FIGURE 1: Identification of novel mammalian TRAPP components. (A) HEK293T cells were transfected with an empty vector (vector) or transfected with either TAP-C2 or TAP-C2L. Lysates were subjected to a two-step affinity purification and fractionated by SDS–PAGE. Bands were excised and subjected to mass spectrometric identification. In some cases, bands were not resolved and the entire eluate was analyzed by mass spectrometry. The bait band refers to either C2 (lane 2) or C2L (lane 3). TTC15/TRAPPC12 is marked with an asterisk since it was not identified in a gel slice but rather following mass spectrometric analysis of a non-gel-resolved protein preparation. Note that the uneven staining of the gel is due to the use of a discontinuous gradient in the resolving portion of the gel. (B) Lysates of HEK293T cells transfected with FLAG-C2L and myc-C2 (lane 1) were treated with preimmune rabbit serum (lane 2) or anti–FLAG IgG (lane 3), and the precipitates were subjected to Western analysis using anti–myc IgG. (C) Eluates following TAP purification were fractionated from cells transfected with an empty plasmid (vector) or with the TAP-C4orf41. The gel was transferred to a PVDF membrane and probed for the presence of the indicated TRAPP proteins. (D) HEK293T cells were transfected with HA-C4orf41. Lysates were incubated with preimmune serum (lane 2), anti-HA (lane 3), or anti-TTC15/C12 (lane 4). Immunoprecipitates were then fractionated by SDS–PAGE and probed for the presence of C2, C2L, C3, C12 or HA (indicating the presence of C4orf41/C11). Inputs representing 10% of the sample precipitated are shown in lane 1.

the high-molecular-weight polypeptides on this gel appear to be present in stoichiometric amounts.

In an effort to confirm the stable association of C4orf41 with TRAPP, we purified the complex using TAP-C4orf41 followed by SDS–PAGE. Numerous TRAPP proteins were identified by Western analysis (Figure 1C).

Although identification of the new TRAPP proteins after TAP purification strongly suggests a stable association with the complex, we sought to confirm this result by coimmunoprecipitation. We therefore precipitated epitope-tagged C11 or endogenous C12 using a commercially available antibody and probed the precipitates for other TRAPP components. As seen in Figure 1D, C4orf41 and TTC-15 interact both with each other and with previously characterized TRAPP subunits, demonstrating by a second method that they are indeed stably associated with the complex. These results firmly establish the newly identified proteins as stable TRAPP interactors. We henceforth designate these new components TRAPPC8 (KIAA1012), TRAPPC11 (C4orf41), and TRAPPC12 (TTC-15), following the precedents from the automatic annotation and the order of their discovery.

C8/KIAA1012 has been automatically annotated as a Trs85p orthologue, but its presence in our multiple purifications confirms it as the Trs85p orthologue experimentally. The mammalian protein is significantly longer than its *S. cerevisiae* counterpart (see Table 1) and displays several short regions of homology. Trs85p has been previously characterized as a yeast TRAPP component and was recently suggested to play a specific role in autophagy in yeast as a component of a discrete TRAPP subassembly (TRAPP III) (Lynch-Day *et al.*, 2010). Interestingly, we find that C8 depletion causes Golgi fragmentation, supporting a role for the mammalian orthologue in ER-to-Golgi trafficking (see below).

C11/gryzun is found in all eukaryotic kingdoms, including fungi, but is absent from *S. cerevisiae* and *Schizosaccharomyces pombe* (Supplemental Figure 1A). The protein contains nonoverlapping regions of homology to both human C10 and *S. cerevisiae* Trs130p (Supplemental Figure 2; Wendler *et al.*, 2010). The importance of C11 in cellular function is evident from the fact that, in zebrafish, a loss-of-function mutation is embryonic lethal (Sadler *et al.*, 2005), whereas *Drosophila* mutants display defects in learning and memory (Dubnau *et al.*, 2003).

C12/TTC-15 contains a tetratricopeptide repeat domain that is well characterized as a protein–protein interaction domain mediating hetero- and self-associations (Lamb *et al.*, 1995). The domain is composed of degenerate repeats of a 34-amino-acid motif, and C12 contains four such repeats (Supplemental Figure 3). The protein is well-conserved through evolution but, like C11, is curiously absent from *S. cerevisiae*. As is the case with C11, however, orthologues are detected in other fungi (Supplemental Figure 1B).

C11 and C12 cofractionate with TRAPP

We next examined the fractionation of the newly identified proteins by size exclusion chromatography. Consistent with our previous results regarding TRAPP organization in mammalian cells (Scrivens *et al.*, 2009), V5-tagged C8 and endogenous C11 and C12 eluted in the same high-molecular-weight fraction as other TRAPP subunits examined, including endogenous C2, C2L, C3, and V5-tagged C10 (Figure 2A). A second peak for V5-C10 was seen and is most likely due to ectopic expression because it caused a shift in the low-molecular-weight pool of C2L (Supplemental Figure 4) and was not seen for the endogenous C10 protein (Yamasaki *et al.*, 2009). Curiously, endogenous C12 was observed to elute in the same high-molecular-weight pool as TRAPP, as well as a 400- to 500-kDa fraction distinct from other TRAPP components. The components of this smaller C12 assembly are currently being characterized.

To further address the role of C11, we examined the effect of depletion of the endogenous protein by siRNA on complex integrity. Interestingly, depletion of C11 (Supplemental Figure 5) resulted in a partial disassembly of the TRAPP complex, as evidenced by a partial redistribution of the C2 signal from the high-molecular-weight to a very-low-molecular-weight fraction and a loss of C12 from the highest molecular weight pool relative to the ~500 kDa fraction (Figure 2B). A minor effect was also observed for C3, though this was more difficult to discern given the large pool of monomeric C3 in unperturbed cells (see Figure 2A) (Loh *et al.*, 2005; Scrivens *et al.*, 2009; Yamasaki *et al.*, 2009). Furthermore, the C11 knockdown affected the levels of C12 but did not significantly alter the levels of C2, C2L, or C3 (Figure 2C). These results indicate that, whereas *S. cerevisiae* can assemble TRAPP (I or II) in the absence of a C11 orthologue, this protein stabilizes the TRAPP complex in mammalian cells.

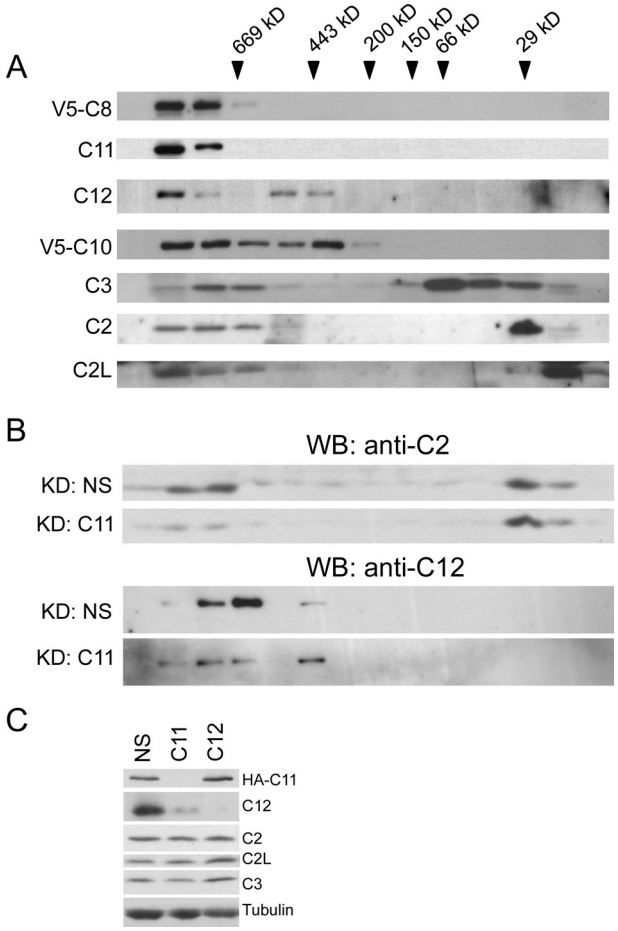

FIGURE 2: Size exclusion chromatography of TRAPP components. (A) Lysates from HEK293T cells left untransfected or transfected with V5-C8 or V5-C10 were fractionated on a Superdex 200 size exclusion column. Fractions (0.5 ml) were collected, and every second fraction was analyzed by Western analysis using antibodies against endogenous C2, C2L, C3, C11, and C12, or anti-V5 to detect transfected C8 or C10. (B) HeLa cells were treated with a nonspecific siRNA (KD: NS) or siRNA against C11 (KD: C11). Lysates were fractionated by size exclusion chromatography as above and subjected to Western analysis using anti–C2 antibody (top two panels) or anti–C12 antibody (bottom two panels). (C) HeLa cells transfected with HA-C11 were treated with a nonspecific siRNA (NS) or siRNA against C11 or C12. Equal amounts of the lysates were analyzed by Western blotting and probed for the presence of tubulin (loading control), C2, C2L, C3, C11 (using anti-HA), and C12.

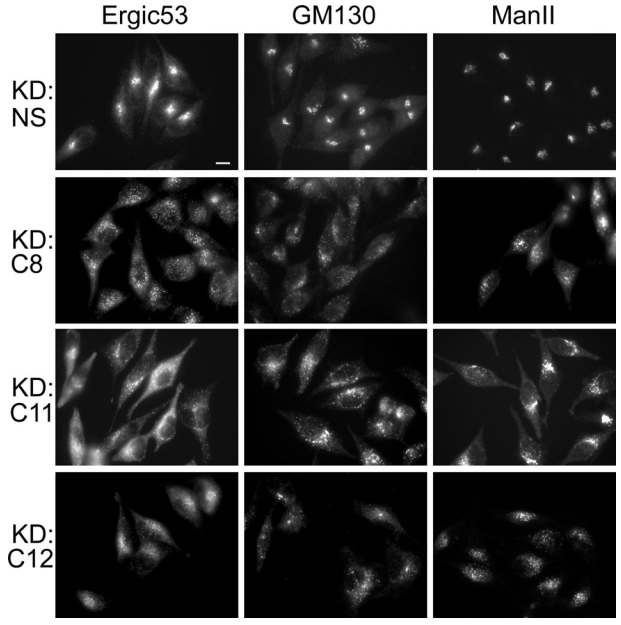

FIGURE 3: Depletion of TRAPPC8, TRAPPC11, or TRAPPC12 results in Golgi dispersal. HeLa cells were treated with nonspecific siRNA or with siRNA against C8, C11, or C12 as indicated. Cells were stained with antibodies against ERGIC53, GM130, and mannosidase II, as indicated. The bar represents 10 μm. Quantitation of the phenotype using GM130 as a marker showed that 73% (n = 125), 88% (n = 43), and 88% (n = 42) of the cells from the C8, C11, and C12 knockdowns, respectively, displayed fragmented Golgi compared with 6% (n = 97), 2% (n = 52), and 2% (n = 52) from the nonspecific siRNA controls, respectively.

Depletion of C8, C11, or C12 by RNAi results in Golgi fragmentation

We previously reported that depletion of C2 and C2L by RNAi in HeLa cells results in Golgi fragmentation, suggestive of a role in ER-to-Golgi trafficking analogous to that characterized for yeast TRAPP I (Scrivens *et al.*, 2009). Although C2 (as a Trs20p orthologue) represents a component of a putative mammalian TRAPP I core, given the proposed role of Trs85p in autophagy, we did not know whether the depletion of its homologue C8, or of C11 and C12 (with no *S. cerevisiae* orthologues), would recapitulate this phenotype.

As was the case with C2 or C2L depletion, RNAi against C8, C11, or C12 resulted in Golgi fragmentation in the form of dispersed punctae, as assessed by indirect immunofluorescence of the ER-to-Golgi intermediate compartment (ERGIC), *cis*- and *medial*-Golgi markers ERGIC53, GM130, and Golgi α-Mannosidase II (Man II), respectively (Figure 3). The C11 knockdown phenotype is consistent with an earlier study showing a similar Golgi phenotype (Wendler *et al.*, 2010). These results imply that the three novel TRAPP-associated proteins function in the early secretory pathway.

C12 displays a punctate and perinuclear localization

Previous studies examining the localization of mammalian TRAPP components have suggested that C3, a core component of the complex, localizes to the transitional ER, whereas C10 and several other subunits were reported to colocalize with early Golgi markers (Yu *et al.*, 2006; Yamasaki *et al.*, 2009). These results prompted us to examine the localization of endogenous C12 using an antibody specific to this subunit. We first used epifluorescence microscopy to validate the C12 antibody in the context of a specific or control knockdown (Figure 4A). The pattern seen in HeLa cells in the absence of C12 knockdown was highly punctate with an obvious concentration of the punctae in the perinuclear region (Figure 4A), reminiscent of that observed for C11 (C4orf41) in *Drosophila* cells (Wendler *et al.*, 2010) and for C3 in NRK cells (Loh *et al.*, 2005). Analysis by maximum projection of confocal images recapitulated this punctate localization, in contrast to the ribbon-like localization observed for Golgi markers and the perinuclear portion of ERGIC53 (Figure 4A).

Examination of individual confocal slices revealed that a small portion of the C12 signal overlapped with that of the ERGIC marker ERGIC53, whereas we observed minimal colocalization with the ERES marker/COP II constituent Sec23a or with the *cis*- and medial Golgi markers GM130 and Man II (Figure 4B). This labeling pattern was maintained upon nocodazole treatment, upon which we observed a small portion of the C12 signal overlapping with ERGIC53,

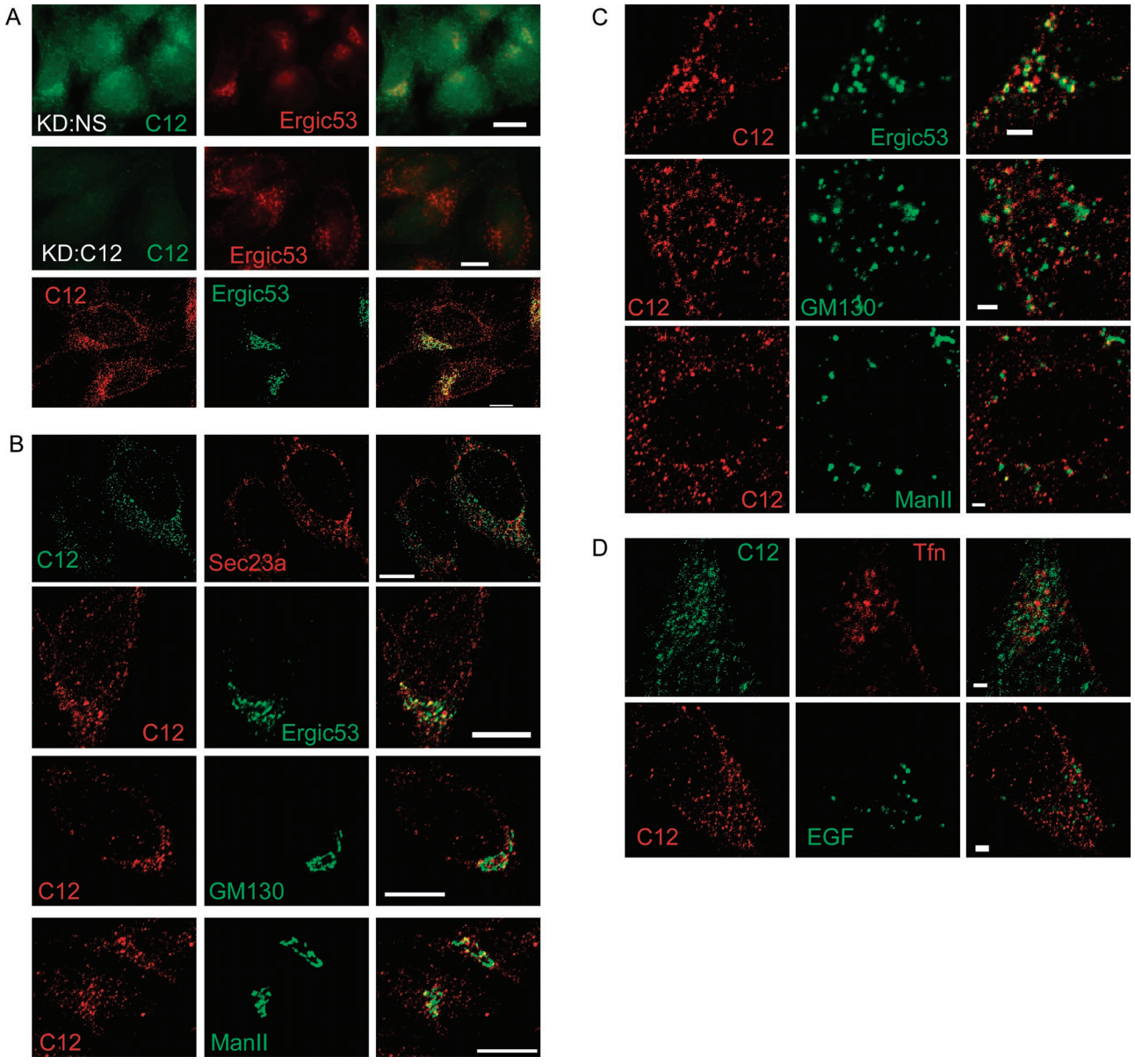

FIGURE 4: Localization of TRAPPC12. (A) HeLa cells were treated with nonspecific (NS; top row) or C12-specific (middle row) siRNAs and stained for C12 and ERGIC53, then visualized by epifluorescence microscopy (upper two rows). Maximum projection of confocal images from NS-treated cells (third row) recapitulates the punctate, perinuclear C12 localization seen by epifluorescence microscopy. (B) Single confocal slices of untreated HeLa cells costained for C12 and Sec23a, ERGIC53, GM130, or Man II. (C) HeLa cells were treated with 10 μM nocodazole for 1 h and then stained with antibodies against C12 and either ERGIC53, GM130, or Man II, as indicated. (D) HeLa cells were serum-starved for 2 h prior to incubation with fluor-tagged EGF or transferrin (Tfn). The scale bar in (A) and (B) represents 10 μm, whereas in (C) and (D) it represents 2 μm.

versus merely in proximity to GM130 and Man II (Figure 4C). The localization of this C12 thus contrasts with the reported localization of C10 following nocodazole treatment, where enhanced colocalization with Golgi markers was observed (Yamasaki *et al.*, 2009).

Given that the yeast TRAPP II components Trs120p and Trs130p have been reported to localize to a late Golgi/early endosomal compartment (Cai *et al.*, 2005), we examined the localization of C12 with respect to internalized, fluorescently labeled epidermal growth factor (EGF) or Transferrin (Tfn). We did not observe significant overlap with either of these endocytic markers (Figure 4D), suggesting that C12 does not localize to early or recycling endosomes.

Depletion of either C11 or C12 perturbs trafficking of ts045-VSV-G-GFP

As components of TRAPP, C11 and C12 are likely involved in anterograde traffic between the ER and the Golgi. The fragmentation of the Golgi observed upon knockdown is indicative of such a role, but to address this notion directly, we examined the effect of C11 and C12 depletion on the trafficking of the temperature-sensitive, fluorophore-tagged VSV-G mutant ts045-VSV-G-GFP. At temperatures above 38°C, this mutant protein is retained in the ER, but upon shifting to the permissive temperature of 32°C, it is efficiently released, first to the ERGIC and then further through the secretory pathway (Bergmann and Singer, 1983; Scales *et al.*, 1997). HeLa cells were

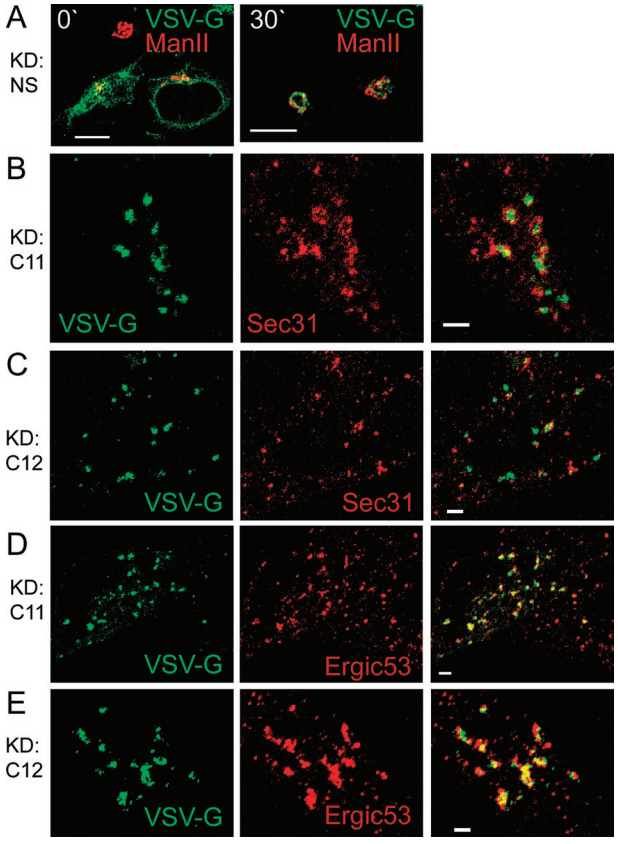

FIGURE 5: Depletion of either TRAPPC11 or TRAPPC12 perturbs ts045-VSV-G-GFP trafficking. HeLa cells were treated with nonspecific siRNA (A) or siRNA against either C11 (B and D) or C12 (C and E). After 48 h, cells were transfected with a plasmid encoding ts045-VSV-G-GFP. Cells were then shifted to 39.5°C for 6 h (A, left) and subsequently incubated at 32°C for 30 min (all other panels). Cells were then stained with anti-Sec31 or anti-ERGIC53, as indicated. The right panels in (B–E) represent merged images from the two panels directly to their left. The scale bar in (A) is 10 μm, and all other bars are 2 μm.

depleted of C11 or C12 using siRNA for 48 h and then transfected with a plasmid containing ts045-VSV-G-GFP (VSV-G). The following day, VSV-G was blocked in the ER by incubation at the restrictive temperature for 6 h. VSV-G was then released by shifting to 32°C for 30 min in the presence of cycloheximide. In cells treated with a nonspecific oligonucleotide, the fluorescent signal appeared in the perinuclear region within 30 min and colocalized with the Golgi marker Man II (Figure 5A). On knockdown of C11 or C12, however, the mutant protein did not traffic to a perinuclear region typical of the Golgi, but rather accumulated in punctate structures (Figure 5, B–E, and Supplemental Figure 7). Confocal microscopy demonstrated that these punctae costain for ERGIC53 (Figure 5, D and E) and are closely apposed to Sec31 (Figure 5, B and C), markers for the ERGIC and ER-exit sites, respectively (Figure 5). These results are consistent with the VSV-G visualized here, representing either cargo at an ER exit site or peripheral ERGIC apposed to an ER exit site, similar to that reported by Mironov *et al.*, 2003.

We previously showed that knockdown of either C2 or C2L results in Golgi fragmentation as evidenced by Man II–positive punctae that also contained ERGIC53 (Scrivens *et al.*, 2009), and in this study, have shown a similar phenotype following knockdown of either C11 or C12. To more formally demonstrate that VSV-G is not merely labeling a functional Golgi mini-stack after a short release, we examined its localization in C11-depleted cells after long incubation times. It has been demonstrated via live-cell imaging that VSV-G reaches the cell surface within ~100 min after release from the ER (Hirschberg *et al.*, 1998; Vasserman *et al.*, 2006). Consistent with the notion that C11-depleted cells are deficient in anterograde trafficking, the VSV-G label remained punctate even 3.5 h after the shift to 32°C (Figure 6, A and B). We postulated that VSV-G had

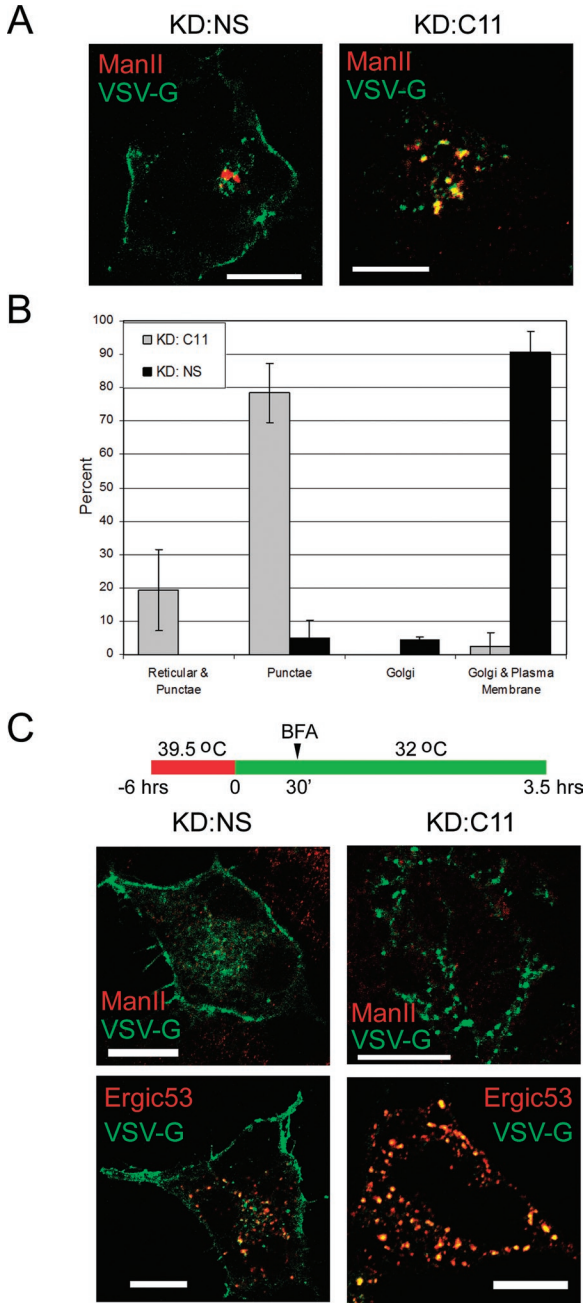

FIGURE 6: ts045-VSV-G-GFP is arrested in a BFA-resistant compartment upon TRAPPC11 depletion. (A) HeLa cells were treated as in Figure 5, except the cells were processed for fluorescence microscopy following 3.5 h at 32°C. Markers examined are indicated in each panel. (B) Quantification of the observed trafficking defect in C11-depleted HeLa cells. Approximately 30 cells per replicate were counted from 3 independent replicates following release from 39.5°C. (C) HeLa cells were treated as in (A), except 30 min into the 32°C incubation, BFA was added to the cultures. The scale bars represent 10 μm.

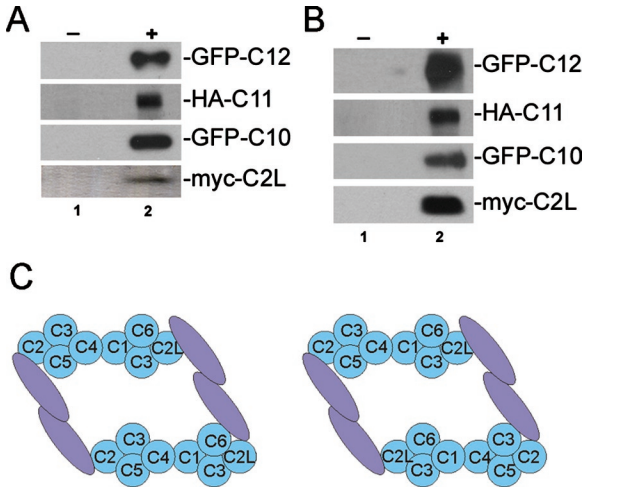

FIGURE 7: Mammalian TRAPP forms oligomers. (A) HEK293T cells were cotransfected with FLAG-C2L/myc-C2L, V5-C10/GFP-C10, V5-C11/HA-C11, or V5-C12/GFP-C12. Lysates were treated with preimmune rabbit serum (lane 1), anti–FLAG (for the C2L transfections), or anti–V5 (for the C10, C11, and C12 transfections) IgG and then probed with anti–myc (for the C2L transfection), anti–GFP (for the C10 and C12 transfections), or anti–HA (for the C11 transfection) IgG. (B) The lysates from (A) were fractionated by gel filtration chromatography. The high-molecular-weight TRAPP-containing fractions were pooled and immunoprecipitated and probed as in (A). (C) A model for the architecture of mammalian TRAPP built from yeast two-hybrid and coimmunoprecipitation data. Subunits shaded in blue are arranged based on the previously published architecture of the subcomplex (Kim *et al.*, 2006). The high-molecular-weight subunits (C8–C12) are represented by a single mauve oval. Given interactions between high–molecular-weight components with proteins at both ends of the TRAPP "core," a network of high-molecular-weight subunit interactions among themselves, and oligomerization of the complex as indicated in (A) and (B), two TRAPP "cores" could be bound via high-molecular-weight subunit interactions in trans. The two models differ with respect to the orientation of the second "core." See the text for details.

failed to reach the Golgi and tested this hypothesis by treating C11-depleted cells with the fungal metabolite brefeldin A (BFA), which causes rapid collapse of the *cis*- and *medial*- Golgi into the ER (Lippincott-Schwartz *et al.*, 1989) and a redistribution of ERGIC53 to ER exit sites or closely associated peripheral ERGIC elements (Saraste and Svensson, 1991; Marie *et al.*, 2009). As shown in Figure 6C, the Man II signal was redistributed to the ER and was barely visible, indicating that retrograde traffic of this marker was not impaired upon C11 depletion. Importantly, both the VSV-G and ERGIC53 punctae were BFA-resistant and remained colocalized. These results are consistent with C11 depletion arresting anterograde trafficking at an early stage, either at ER exit sites or closely apposed peripheral ERGIC (see Figure 5, B–E).

Mapping of mammalian TRAPP interactions

Although our mass spectrometry, immunoprecipitation, and Western blotting data strongly support the interaction of C8, C11, and C12 with TRAPP in mammalian cells, they do not provide architectural information about mammalian TRAPP. To begin to address this, we mapped the binary interactions of each of the TRAPP subunits by yeast two-hybrid.

We sought to assemble a complete set of TRAPP components. Earlier reports identified several isoforms of the C6 subunit, including two different C6a isoforms as well as C6b (Kim *et al.*, 2005; Kummel *et al.*, 2005, 2008), and we previously identified C2L by its similarity to C2 (Scrivens *et al.*, 2009). To ensure that all possible TRAPP subunits were included in this study, we mined GenBank for TRAPP-related proteins. Indeed, we identified a protein annotated as Bet3-like (using our convention of subunit nomenclature of the mammalian orthologues, we will refer to this protein as C3L). C3 and C3L are clearly related, displaying ~60% identity at the amino acid level (Supplemental Figure 8A). Key features previously identified on C3, including residues that make up a basic patch on one surface and a cysteine residue that can be acylated, are preserved in C3L. Strikingly, although C3 and C3L are nearly identical in size, C3L has a predicted isoelectric point (pI) of 8.11, whereas C3 is considerably more acidic with a pI of 4.88. This difference is readily seen at the carboxy terminus: whereas the carboxy terminus of C3 is acidic, the carboxy terminus of C3L is highly basic.

To confirm that C3L is capable of interacting with TRAPP, a FLAG-tagged version was expressed in HEK293T cells, and lysates were immunoprecipitated with antibodies against several TRAPP proteins and then probed for the presence of FLAG-C3L. As shown in Supplemental Figure 8B, FLAG-C3L coprecipitated with C2, C10, C11, and C12, confirming that it is a TRAPP-associated protein that should be included in our binary interaction map.

For the yeast two-hybrid analysis, each TRAPP subunit was tested in both the bait and prey vectors against all subunits listed in Table 1. All previously identified interactions based on earlier structural work with some of the mammalian subunits (Kim *et al.*, 2006) were recapitulated in our extensive binary interaction map, suggesting that this is a valid means to assess interacting partners within this complex (Table 3). The strongest interactions were seen between C2/C2L/C6 and the high-molecular-weight proteins C10, C11, and C12. In addition, the high-molecular-weight proteins appear to have extensive and strong interactions among themselves. These data support a model of mammalian TRAPP in which the high-molecular-weight proteins associate with each other and with one or both ends of the complex via interactions with C6, C2L, and/or C2 (see Figure 7C).

Human TRAPP forms oligomers

Several results prompted us to examine whether human TRAPP forms oligomers. First, some interactions seen by the yeast two-hybrid studies above were not seen in the crystal structure. One example is the C4–C2 interaction, which was unexpected since these subunits are separated by both C3 and C5 (Kim *et al.*, 2006). Interestingly, this interaction was also noted for the yeast homologues Trs20p and Trs23p (S.B. and M.S., unpublished data). Second, the size of TRAPP by gel filtration is larger than expected for the sum of its subunits. This is demonstrated by its elution at or near the void volume using a column with a nominal cutoff of 1300 kDa (Superdex 200) (Figure 2; Loh *et al.*, 2005; Kummel *et al.*, 2008; Scrivens *et al.*, 2009; Yamasaki *et al.*, 2009). To investigate whether these results may be due to oligomerization of the complex, HEK293T cells were cotransfected with individual TRAPP proteins bearing two different epitope tags. Lysates were prepared, and the subunit of interest was precipitated with an antibody against one of the tags. The immunoprecipitate was then probed for the presence of the other tag, indicating that the two proteins either associate together or are in the same complex. This experiment was performed for tagged versions of C2L, C10, C11, and C12. As seen in Figure 7A, a tagged version of each subunit precipitated the other tagged version of the same subunit. Because several of these proteins have non-TRAPP-associated pools (see Figure 2), the coimmunoprecipitation experiment was performed on a TRAPP-enriched,

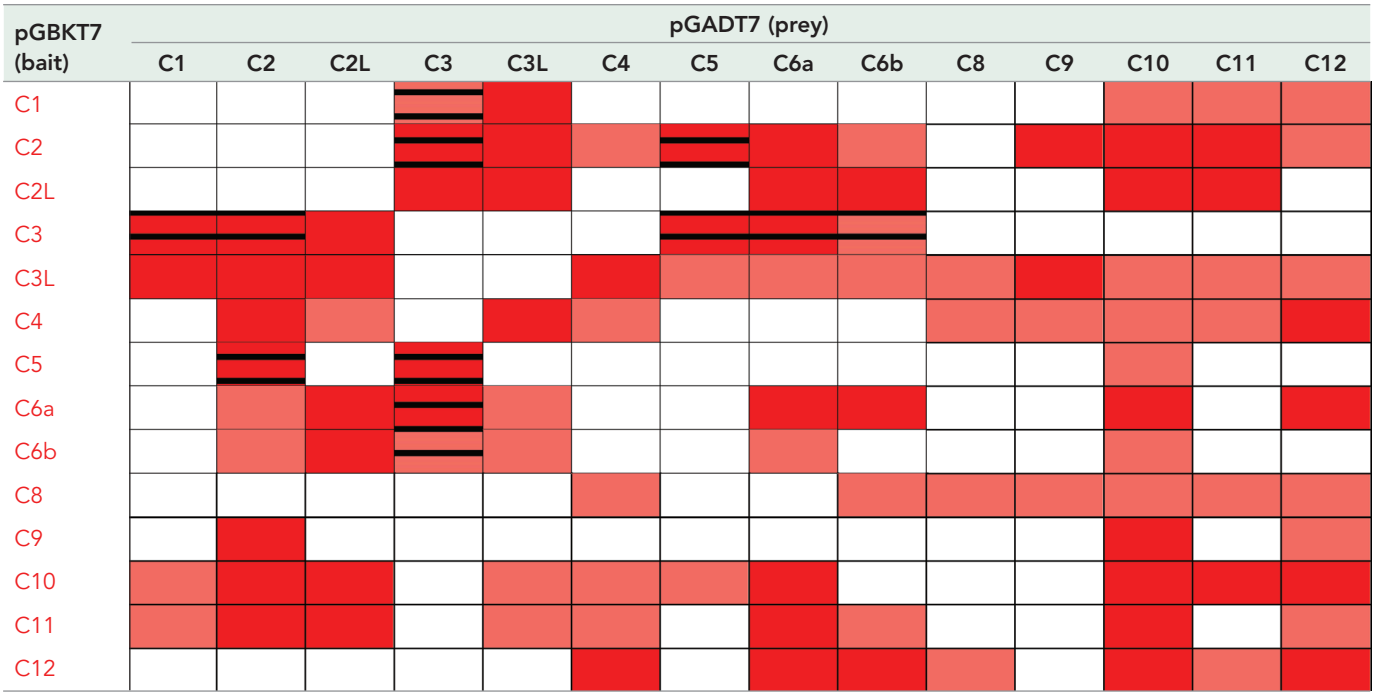

Subunits in red are in the bait vector, whereas those in black are in the prey vector.
Dark red, QDO; light red, TDO; horizontal bars, interactions seen in crystal structure (Kim *et al.*, 2006).

TABLE 3: Summary of binary yeast two-hybrid interactions.

high-molecular-weight fraction by first fractionating the lysate by size exclusion chromatography. Again, for each subunit examined, one tagged version of the TRAPP protein coprecipitated the other tagged version of the same protein (Figure 7B). Collectively, these results indicate that TRAPP forms oligomers in human cells.

DISCUSSION

Although yeast TRAPP is increasingly well-characterized, the components and function of mammalian TRAPP are less defined. The similarity of the C2- and C2L-TAP-purified TRAPP complexes (Figure 1) suggests that we are likely to have discovered most, if not all, mammalian TRAPP components through this methodology. Vesicle trafficking in *S. cerevisiae* and mammalian cells is characterized not only by conserved molecular assemblies and pathways, but by distinct differences between organelle structure and function. *S. cerevisiae*, for example, need to coordinate membrane traffic to a large vacuole, which is absent in mammalian cells. Likewise, differences are seen in Golgi organization, presence or absence of the ERGIC, and distribution of ER exit sites. Distinct trafficking steps in yeast are mediated by discrete subassemblies of TRAPP, with TRAPP I mediating ER-to-Golgi and TRAPP II mediating late Golgi vesicle trafficking. In contrast, we and others (Loh *et al.*, 2005; Yu *et al.*, 2006; Kummel *et al.*, 2008; Yamasaki *et al.*, 2009) have shown that no TRAPP I equivalent (a complex composed of C1–C6) is present in mammalian cells, but rather that the fundamental unit of TRAPP is a much larger assembly. This raises the question of whether and how mammalian TRAPP, like yeast TRAPP, mediates discrete trafficking events, which is addressed below.

Together with the extensive yeast two-hybrid analysis, we present a model for the architecture of mammalian TRAPP (Figure 7C). Based on our most stringent growth criterion in the yeast two-hybrid analysis, we speculate that the C2 and C2L ends of the TRAPP core (Figure 7C, blue circles) mediate interactions with the high-molecular-weight subunits (Figure 7C, mauve ovals). Oligomers may form by association of two or more such units. Yeast two-hybrid data and the partial destabilization of TRAPP observed upon C11 knockdown suggest that C11 may mediate the interactions between the TRAPP core (through C2L and C6) and other large TRAPP subunits. Preliminary data on the interactions of various domains of C11 support this notion (B.N. and M.S., unpublished observation). The orientation of the two TRAPP cores is unclear, and they may align either parallel or antiparallel as depicted in our model. However, either model allows for interactions between subunits that were not seen in the crystal structure of the core by interactions between two or more cores of the TRAPP oligomer.

The most closely related yeast complex to human TRAPP is TRAPP II, whose architecture was recently reported (Yip *et al.*, 2010). In TRAPP II, the core is flanked by the high-molecular-weight subunits Trs130p and Trs120p. Dimerization was mediated by interactions between either of these two high-molecular-weight subunits and Trs65p. Although similar to the yeast TRAPP II architecture, our model differs in several respects. First, higher eukaryotes do not have a Trs65p homologue (see Table 1), and therefore oligomerization must be mediated by another subunit. Second, higher eukaryotes contain C11 and C12, proteins that are not found in *S. cerevisiae*. Therefore the "caps" on the ends of the TRAPP core may vary quite significantly from those of yeast TRAPP II. The subunits comprising the caps in human TRAPP may provide functions to the complex that are not needed in *S. cerevisiae*. Finally, given the similar phenotype between C8, C11, C12, C2, and C2L knockdowns, our model suggests that all of these subunits may be present in the oligomers of TRAPP, whereas the orthologues of C8 and C2L (Trs85p and Tca17p, respectively) were not detected in TRAPP II purified with tagged Trs120p (Yip *et al.*, 2010). Our model is consistent with a previous report demonstrating that C6a and C6b cofractionate by size exclusion chromatography (Kummel *et al.*, 2008). Because neither the crystal structure of yeast nor mammalian TRAPP suggested

the presence of multiple copies of C6, we suggest that cofractionation of two isoforms of this subunit is due to oligomerization of the complex.

Oligomerization of TRAPP can give rise to complexes with variable components in any one of several positions (i.e., C6a/b, C3/C3L) and might allow for a combinatorial diversification of TRAPP function, perhaps regulating cell-specific activities. Indeed, C3L appears to have a limited expression profile (http://www.genecards.org/cgi-bin/carddisp.pl?gene=BET3L&search=bet3l) relative to C3, suggesting a functional diversification. Intriguingly, residues previously implicated as critical for Ypt1p GEF activity in Bet3p are conserved in C3 but not in C3L (Cai *et al.*, 2008).

What, then, is the function of the complex? Localization of subunits by fluorescence microscopy has proven difficult due to the large soluble pools of the proteins. However, C3 was reported to be localized to ER exit sites, whereas C2, C4, and C10 were reported to be bound to COP I vesicles at or near the Golgi (Yu *et al.*, 2006; Yamasaki *et al.*, 2009). Here we report that C12 is largely found in punctae throughout the cell and knockdowns of either C11 or C12 arrest a cargo protein in a BFA-resistant compartment. It was recently suggested that such a BFA-resistant compartment represents peripheral elements of the ERGIC in close association with the ER (Marie *et al.*, 2009). Furthermore, C3 was proposed to be involved in formation of the ERGIC (Yu *et al.*, 2006). Together with the present study, we suggest that TRAPP functions either at ER exit sites or at peripheral ERGIC (BFA-resistant) elements. A defect at the ERGIC may be expected to have an indirect effect on the ability of cargo to properly exit the ER. It remains a possibility that TRAPP may function at both stages (ER exit and early ERGIC) in the early secretory pathway. This notion is supported by several pieces of evidence. Yeast TRAPP acts as a GEF for Ypt1p and precipitation of C10 coprecipitates a Rab1 GEF (Jones *et al.*, 2000; Wang *et al.*, 2000; Yamasaki *et al.*, 2009). A function for activated Rab1 during vesicle budding has been reported previously (Allan *et al.*, 2000), and therefore its GEF would be expected to associate with budding vesicles at ER exit sites. Thus, TRAPP, or a subset of TRAPP proteins, may play an as yet undefined role during vesicle budding accounting for a defect in cargo exit from the ER as we report. Given its well-documented role as a vesicle tether in yeast, the complex may in fact migrate on ERGIC membranes to the Golgi, where it performs a second (tethering) function. The localization of subunits on Golgi-derived COP I vesicles may represent a means to recycle the complex back to ERGIC membranes and, analogous to yeast, may thus function in traffic to the early Golgi. The necessarily dynamic nature of the membrane association of TRAPP proteins could account for differences in their reported localization. Alternatively, C12 appears to fractionate in a second pool distinct from other TRAPP proteins and its localization may be linked to this pool.

C8 (KIAA1012) was found to copurify with TAP-C3 (Gavin *et al.*, 2002). Its copurification with several other TRAPP components and its implication in vesicle trafficking as demonstrated in this study confirm that it is a bona fide TRAPP subunit. Although its yeast orthologue Trs85p was suggested to be in a complex distinct from TRAPP I and TRAPP II that functions in autophagy (Lynch-Day *et al.*, 2010), our study clearly links the mammalian protein to the early secretory pathway. Although our results indicate a general role for C8 in membrane trafficking, they do not preclude a second role for this protein in autophagy in mammals.

Recombinant expression of the yeast equivalent of C1–C6 resulted in a stable, functional core complex, whereas recombinant expression of the mammalian proteins did not (Kim *et al.*, 2006). It was previously speculated that the recombinant mammalian TRAPP core required other subunits to facilitate its stable assembly (Sacher *et al.*, 2008). Our identification of a number of new proteins, the loss of two of which (C11 or C12) appears to partially destabilize the complex in vivo, supports this notion. A detailed analysis of the structure of human TRAPP will help to explain this phenomenon.

MATERIALS AND METHODS

Yeast two hybrid

Modified pGADT7 and pGBKT7 plasmids containing TRAPP subunits were transformed into AH109 and Y187 yeast, respectively. Mating was performed on YPD agar plates, and mating efficiency was tested on –leucine/–tryptophan agar plates. Interactions were assessed on –leucine/–tryptophan/–histidine (without or with 3-amino-1,2,4-triazole) and on –leucine/–tryptophan/–histidine/–adenine plates.

ts045-VSV-G-GFP trafficking assay

HeLa cells were plated on glass coverslips in DMEM supplemented with 10% fetal bovine serum (FBS). One hour prior to transfection, DMEM was removed and replaced with Optimem. Cells were knocked down with 12 pmol siRNA per well in a 12-well dish. Approximately 20 h after transfection, 1 ml DMEM + 10% FBS was added to each well. One hour later, the medium was exchanged for fresh DMEM + 10% FBS and the dishes were returned to the 37°C incubator for 24 h.

ts045-VSV-G-GFP transfection

VSV-G transfection was performed ~48 h after the start of the knockdown. Each well was transfected with 0.4 µg pEGFP-VSV-G (ts045) (Addgene, Cambridge, MA) using Lipofectamine 2000 (Invitrogen, Carlsbad, CA). Plates were returned to the 37°C incubator for ~18 h.

Temperature shifts

Dishes were placed in a 39.5°C incubator for 6.5 h to induce ER retention of the ts045-VSV-G-GFP. At this point, control cells were fixed on ice. The remainder of the cells were shifted to 32°C by replacement of medium with 32°C DMEM + 10% FBS containing 10 µg/ml cycloheximide and transferred to a 32°C incubator for 30 min. Cells were fixed after 30 min at 32°C, or were left for an additional 3 hours with or without 5 µg/ml BFA. Following release, all cells were prepared for microscopy as described below.

Fluorescence microscopy

Cells containing ts045-VSV-G-GFP fusions were fixed with 4% paraformaldehyde in phosphate-buffered saline (PBS), washed thoroughly with PBS, then permeabilized by addition of cold methanol prior to immunofluorescence labeling. For labeling of TRAPPC12/TTC-15 and Sec23a or endosomes (EGF-Alexa 488 or Tfn-Alexa 546), HeLa cells were fixed with 4% paraformaldehyde in PBS, washed extensively, then permeablized with 0.2% Triton X-100 in PBS (Tfn, Sec23a) or 0.05% digitonin (EGF). For endosome staining, HeLa cells were serum-starved for 2 h prior to a 15-min incubation with fluor-tagged Tfn or EGF. All other cells were fixed and permeabilized with −80°C methanol:acetone (4:1). Fixative was removed and cells were blocked 2% FBS, 2% bovine serum albumin (BSA), and 0.2% fish skin gelatin. Primary antibodies were diluted in blocking buffer at the following concentrations: Sec31a 1:250 (monoclonal, BD diagnostics, catalogue #612350); ERGIC53 1:125 (rabbit, Sigma catalogue #E1031); GM130 1:5000 (ML07, rabbit) 1:200 (4A3, kind gifts of Martin Lowe); Golgi MannosidaseII 1:500 (rabbit, kind gift of Kelley Moremen); TRAPPC12/TTC-15 1:100 (mouse polyclonal, Abnova catalogue #H00051112-B01); Sec23a 1:500 (rabbit

polyclonal serum, kind gift of Randy Schekman); Sar1b 1:100 (rabbit polyclonal, Assay Biotech catalogue #C16030). Secondary antibodies (Alexa488- or Alexa546-labeled anti–mouse or anti–rabbit secondary antibodies; Invitrogen) were diluted in blocking buffer containing 4′,6-diamidino-2-phenylindole (DAPI). Golgi fragmentation was assessed by epifluorescence microscopy using a Zeiss Axioplan microscope. VSV-G trafficking was monitored on fixed cells using a Leica TCS SP2 confocal microscope.

Tandem affinity purification

TAP-tagged TRAPPC2, TRAPPC2L, or TRAPPC11 were expressed in HEK293T cells. Cells were transfected with the expression plasmid and harvested 48 hours after transfection. TAP-tagged proteins were bound to IgG sepharose (GE Healthcare, Little Chalfont, UK) in batch before treatment with Tobacco Etch Virus (TEV) protease. TEV protease–treated eluates were bound to calmodulin agarose beads (New England Biolabs, Ipswich, MA), washed and then eluted in 50 mM Tris, pH 6.8, 25 mM EGTA. Elutions were subjected to SDS–PAGE followed by silver staining or visualization with Bio-Safe coomassie (Bio-Rad, Hercules, CA), bands were excised, and identified by mass spectrometry.

Coimmunoprecipitation

Coimmunoprecipitations were performed on 500 µg protein with 1 µg antibody. Immune complexes were captured onto either protein G- or protein A-agarose. Beads were washed three times with lysis buffer (150 mM NaCl, 0.5 mM EDTA, 50 mM Tris, pH 7.2, 1% Triton X-100, 1 mM dithiothreitol [DTT], 1× Complete EDTA-free protease inhibitor) and resuspended with 1× Laemmli sample buffer. Protein samples were boiled for 2 min at 95°C, centrifuged at maximum speed for 2 min, and fractionated by SDS–PAGE.

ACKNOWLEDGMENTS

We are grateful to Kurt Dejgaard at the McGill University Proteomics Core Facility, Heng Jiang for performing the initial mass spectrometric analyses and Anne-Claude Gingras, Arnold Kristof, Martin Lowe, Peter McPherson, Kelley Moreman, Randy Sheckman, and Reginald Storms for reagents used in this study. We are also grateful to members of the Sacher laboratory for many helpful discussions. This work was supported by grants from the Canadian Institutes of Health Research (CIHR), the Natural Sciences and Engineering Research Council, and the Canada Foundation for Innovation Leaders Opportunity Fund. M.S. is a recipient of a CIHR New Investigator Award and a member of the Groupe de Recherche Axé sur la Structure des Protéines (GRASP).

REFERENCES

Allan BB, Moyer BD, Balch WE (2000). Rab1 recruitment of p115 into a cis-SNARE complex: programming budding COPII vesicles for fusion. Science 289, 444–448.

Bergmann JE, Singer SJ (1983). Immunoelectron microscopic studies of the intracellular transport of the membrane glycoprotein (G) of vesicular stomatitis virus in infected Chinese hamster ovary cells. J Cell Biol 97, 1777–1787.

Bonifacino JS, Glick BS (2004). The mechanisms of vesicle budding and fusion. Cell 116, 153–166.

Cai H, Yu S, Menon S, Cai Y, Lazarova D, Fu C, Reinisch K, Hay JC, Ferro-Novick S (2007). TRAPPI tethers COPII vesicles by binding the coat subunit Sec23. Nature 445, 941–944.

Cai H, Zhang Y, Pypaert M, Walker L, Ferro-Novick S (2005). Mutants in trs120 disrupt traffic from the early endosome to the late Golgi. J Cell Biol 171, 823–833.

Cai Y *et al*. (2008). The structural basis for activation of the Rab Ypt1p by the TRAPP membrane-tethering complexes. Cell 133, 1202–1213.

Cox R, Chen SH, Yoo E, Segev N (2007). Conservation of the TRAPPII-specific subunits of a Ypt/Rab exchanger complex. BMC Evol Biol 7, 12.

Dubnau J *et al*. (2003). The staufen/pumilio pathway is involved in Drosophila long-term memory. Curr Biol 13, 286–296.

Gavin AC *et al*. (2002). Functional organization of the yeast proteome by systematic analysis of protein complexes. Nature 415, 141–147.

Gedeon AK, Colley A, Jamieson R, Thompson EM, Rogers J, Sillence D, Tiller GE, Mulley JC, Gecz J (1999). Identification of the gene (SEDL) causing X-linked spondyloepiphyseal dysplasia tarda. Nat Genet 22, 400–404.

Gedeon AK *et al*. (2001). The molecular basis of X-linked spondyloepiphyseal dysplasia tarda. Am J Hum Genet 68, 1386–1397.

Hirschberg K, Miller CM, Ellenberg J, Presley JF, Siggia ED, Phair RD, Lippincott-Schwartz J (1998). Kinetic analysis of secretory protein traffic and characterization of golgi to plasma membrane transport intermediates in living cells. J Cell Biol 143, 1485–1503.

Jones S, Newman C, Liu F, Segev N (2000). The TRAPP complex is a nucleotide exchanger for Ypt1 and Ypt31/32. Mol Biol Cell 11, 4403–4411.

Kim MS, Yi MJ, Lee KH, Wagner J, Munger C, Kim YG, Whiteway M, Cygler M, Oh BH, Sacher M (2005). Biochemical and crystallographic studies reveal a specific interaction between TRAPP subunits Trs33p and Bet3p. Traffic 6, 1183–1195.

Kim YG, Raunser S, Munger C, Wagner J, Song YL, Cygler M, Walz T, Oh BH, Sacher M (2006). The architecture of the multisubunit TRAPP I complex suggests a model for vesicle tethering. Cell 127, 817–830.

Kummel D, Muller JJ, Roske Y, Misselwitz R, Bussow K, Heinemann U (2005). The structure of the TRAPP subunit TPC6 suggests a model for a TRAPP subcomplex. EMBO Rep 6, 787–793.

Kummel D, Oeckinghaus A, Wang C, Krappmann D, Heinemann U (2008). Distinct isocomplexes of the TRAPP trafficking factor coexist inside human cells. FEBS Lett 582, 3729–3733.

Lamb JR, Tugendreich S, Hieter P (1995). Tetratrico peptide repeat interactions: to TPR or not to TPR? Trends Biochem Sci 20, 257–259.

Lippincott-Schwartz J, Yuan LC, Bonifacino JS, Klausner RD (1989). Rapid redistribution of Golgi proteins into the ER in cells treated with brefeldin A: evidence for membrane cycling from Golgi to ER. Cell 56, 801–813.

Loh E, Peter F, Subramaniam VN, Hong W (2005). Mammalian Bet3 functions as a cytosolic factor participating in transport from the ER to the Golgi apparatus. J Cell Sci 118, 1209–1222.

Lynch-Day MA, Bhandari D, Menon S, Huang J, Cai H, Bartholomew CR, Brumell JH, Ferro-Novick S, Klionsky DJ (2010). Trs85 directs a Ypt1 GEF, TRAPPIII, to the phagophore to promote autophagy. Proc Natl Acad Sci USA 107, 7811–7816.

Marie M, Dale HA, Sannerud R, Saraste J (2009). The function of the intermediate compartment in pre-Golgi trafficking involves its stable connection with the centrosome. Mol Biol Cell 20, 4458–4470.

Meiling-Wesse K, Epple UD, Krick R, Barth H, Appelles A, Voss C, Eskelinen EL, Thumm M (2005). Trs85 (Gsg1), a component of the TRAPP complexes, is required for the organization of the preautophagosomal structure during selective autophagy via the Cvt pathway. J Biol Chem 280, 33669–33678.

Mironov AA *et al*. (2003). ER-to-Golgi carriers arise through direct en bloc protrusion and multistage maturation of specialized ER exit domains. Dev Cell 5, 583–594.

Montpetit B, Conibear E (2009). Identification of the novel TRAPP associated protein Tca17. Traffic 10, 713–723.

Morozova N, Liang Y, Tokarev AA, Chen SH, Cox R, Andrejic J, Lipatova Z, Sciorra VA, Emr SD, Segev N (2006). TRAPPII subunits are required for the specificity switch of a Ypt-Rab GEF. Nat Cell Biol 8, 1263–1269.

Nazarko TY, Huang J, Nicaud JM, Klionsky DJ, Sibirny AA (2005). Trs85 is required for macroautophagy, pexophagy and cytoplasm to vacuole targeting in Yarrowia lipolytica and Saccharomyces cerevisiae. Autophagy 1, 37–45.

Sacher M, Barrowman J, Schieltz D, Yates JR III, Ferro-Novick S (2000). Identification and characterization of five new subunits of TRAPP. Eur J Cell Biol 79, 71–80.

Sacher M, Barrowman J, Wang W, Horecka J, Zhang Y, Pypaert M, Ferro-Novick S (2001). TRAPP I implicated in the specificity of tethering in ER-to-Golgi transport. Mol Cell 7, 433–442.

Sacher M, Jiang Y, Barrowman J, Scarpa A, Burston J, Zhang L, Schieltz D, Yates JR III, Abeliovich H, Ferro-Novick S (1998). TRAPP, a highly conserved novel complex on the cis-Golgi that mediates vesicle docking and fusion. EMBO J 17, 2494–2503.

Sacher M, Kim YG, Lavie A, Oh BH, Segev N (2008). The TRAPP Complex: Insights into its Architecture and Function. Traffic 9, 2032–2042.

Sadler KC, Amsterdam A, Soroka C, Boyer J, Hopkins N (2005). A genetic screen in zebrafish identifies the mutants vps18, nf2 and foie gras as models of liver disease. Development 132, 3561–3572.
Saraste J, Svensson K (1991). Distribution of the intermediate elements operating in ER to Golgi transport. J Cell Sci 100, Pt 3415–430.
Scales SJ, Pepperkok R, Kreis TE (1997). Visualization of ER-to-Golgi transport in living cells reveals a sequential mode of action for COPII and COPI. Cell 90, 1137–1148.
Scrivens PJ, Shahrzad N, Moores A, Morin A, Brunet S, Sacher M (2009). TRAPPC2L is a novel, highly conserved TRAPP-interacting protein. Traffic 10, 724–736.
Shaw MA, Brunetti-Pierri N, Kadasi L, Kovacova V, Van ML, De BD, Salerno M, Gecz J (2003). Identification of three novel SEDL mutations, including mutation in the rare, non-canonical splice site of exon 4. Clin Genet 64, 235–242.
Tiller GE, Hannig VL, Dozier D, Carrel L, Trevarthen KC, Wilcox WR, Mundlos S, Haines JL, Gedeon AK, Gecz J (2001). A recurrent RNA-splicing mutation in the SEDL gene causes X-linked spondyloepiphyseal dysplasia tarda. Am J Hum Genet 68, 1398–1407.
Vasserman G, Magal LG, Shepshelovich J, Elifaz E, Hirschberg K (2006). Processing of VSVG protein is not a rate-limiting step for its efflux from the Golgi complex. Biochem Biophys Res Commun 351, 689–694.
Wang W, Sacher M, Ferro-Novick S (2000). TRAPP stimulates guanine nucleotide exchange on Ypt1p. J Cell Biol 151, 289–296.
Wendler F, Gillingham AK, Sinka R, Rosa-Ferreira C, Gordon DE, Franch-Marro X, Peden AA, Vincent JP, Munro S (2010). A genome-wide RNA interference screen identifies two novel components of the metazoan secretory pathway. EMBO J 29, 304–314.
Yamasaki A, Menon S, Yu S, Barrowman J, Meerloo T, Oorschot V, Klumperman J, Satoh A, Ferro-Novick S (2009). mTrs130 is a component of a mammalian TRAPPII complex, a Rab1 GEF that binds to COPI-coated vesicles. Mol Biol Cell 20, 4205–4215.
Yip CK, Berscheminski J, Walz T (2010). Molecular architecture of the TRAPPII complex and implications for vesicle tethering. Nat Struct Mol Biol 17, 1298–1304.
Yu S, Satoh A, Pypaert M, Mullen K, Hay JC, Ferro-Novick S (2006). mBet3p is required for homotypic COPII vesicle tethering in mammalian cells. J Cell Biol 174, 359–368.